frontiers in Astronomy and Space Sciences

ORIGINAL RESEARCH
published: 04 May 2021
doi: 10.3389/fspas.2021.641067

Thionitroxyl Radical (H_2NS) Isomers: Structures, Vibrational Spectroscopy, Electronic States and Photochemistry

*Mahmoud Jarraya[1,2], Saida Ben Yaghlane[2], Raimund Feifel[3], Roberto Linguerri[1] and Majdi Hochlaf[1]**

[1] Université Gustave Eiffel, COSYS/LISIS, 5 Bd Descartes 77454, Champs sur Marne, France, [2] Faculté des Sciences de Tunis, Laboratoire de Spectroscopie Atomique, Moléculaire et Applications – LSAMA, Université de Tunis El Manar, Tunis, Tunisia, [3] Department of Physics, University of Gothenburg, Origovägen 6B, Gothenburg, Sweden

The thionitroxyl radical (H_2NS) isomers are characterized using advanced *ab initio* methodologies. Computations are done using standard and explicitly correlated coupled cluster, CASSCF and MRCI approaches in conjunction with large basis sets, extrapolated to the complete basis set (CBS) limit. The lowest electronic states of different isomers are mapped along the stretching coordinates, thereby confirming the existence of the four already known ground state structures, namely H_2NS, H_2SN, *cis*-HNSH and *trans*-HNSH. Also, it is shown that only the lowest electronic excited states are stable, whereas the upper electronic states may undergo unimolecular decomposition processes forming H + HNS/HSN or the HN + SH or N + H_2S or S + NH_2 fragments. These data allow an assignment of the deep blue glow observed after reactions between "active nitrogen" and H_2S at the beginning of the XXth century. For stable species, a set of accurate structural and spectroscopic parameters are provided. Since small nitrogen-sulfur molecular species are of astrophysical relevance, this work may help for identifying the thionitroxyl radical isomers in astrophysical media and in the laboratory.

Keywords: ab intio calculations, electronic state calculations, nitrogen sulfur compounds, vibrational spectroscopy, equilibrium structure

OPEN ACCESS

Edited by:
Ryan C. Fortenberry, University of Mississippi, United States

Reviewed by:
Tarek Trabelsi, University of Pennsylvania, United States
Maria Luisa Senent Diez, Instituto de Estructura de la Materia (IEM), Spain

***Correspondence:**
Majdi Hochlaf
hochlaf@univ-mlv.fr
orcid.org/0000-0002-4737-7978

Specialty section:
This article was submitted to Astrochemistry, a section of the journal Frontiers in Astronomy and Space Sciences

Received: *13 December 2020*
Accepted: *23 March 2021*
Published: *04 May 2021*

Citation:
Jarraya M, Ben Yaghlane S, Feifel R, Linguerri R and Hochlaf M (2021) Thionitroxyl Radical (H_2NS) Isomers: Structures, Vibrational Spectroscopy, Electronic States and Photochemistry. Front. Astron. Space Sci. 8:641067. doi: 10.3389/fspas.2021.641067

INTRODUCTION

To date, several molecular species containing H, N and S atoms are identified in astrophysical media. These include the Galactic center cloud Sgr B2, cold dark clouds, R Andromedae, circumstellar envelopes of evolved stars, regions of massive star formation, planetary atmospheres, brown dwarfs, stellar atmospheres, and comae (Espin, 1890; Neugebauer et al., 1965; Wöhl, 1971; Gottlieb et al., 1975; Meyer and Roth, 1991; van Dishoeck et al., 1993; Wagenblast et al., 1993; McGonagle et al., 1994; McGonagle and Irvine, 1997; Irvine et al., 2000; Yamamura et al., 2000; Ziurys, 2006; Phuong et al., 2018). The list of identified species contains the NS, SH, NH, and NH_2 radicals as well as the H_2S molecule. Other species are also very likely to be present there, such as HSN/HNS and their ions (Ben Yaghlane et al., 2014; Ajili et al., 2016; Trabelsi et al., 2016). In these media, these molecules and the H, N, and S atoms may undergo complex chemistry that may lead to the formation of larger molecular species, already detected or possibly present. All of them are closely related to the molecule investigated here, i.e., the thionitroxyl radical (H_2NS), since they may be involved in its formation or fragmentation.

At the beginning of the XXth century, Strutt, Fowler and Vaidya (Strutt and Fowler, 1912; Strutt, 1913; Fowler and Vaidya, 1931) investigated the reactions of "active nitrogen" with hydrogen sulfide (i.e., N + H_2S) producing NS + H_2. They suggested that these products are formed by decomposition of an N.H_2S tetratomic intermediate. These findings were confirmed in 1960 by Westbury and Winkler (1960) who studied the kinetics of such processes in the 85–440°C temperature range. A deep blue glow was observed in the reaction flame, attributed *a priori* to the N.H_2S long-lived intermediate. In the literature, no solid confirmation of this assignment is found.

In the laboratory, two isomers of the thionitroxyl radical (namely HNSH and H_2SN) and their positively- and negatively-charged ions were detected in 1994 by a combination of collisional activation and neutralization-reionization mass spectrometry, complemented by theoretical computations based on Möller-Plesset (MP2 and MP4) approaches (Nguyen et al., 1994). These computations showed that the most stable [H,H,N,S] species corresponds to H_2NS (C_{2v} symmetry) and not to the already detected HNSH and H_2SN isomers. In 1998, the most stable [H,H,N,S] form was observed by Habara et al. (1998) using source-modulation and Fourier-transform microwave spectrometers. These authors recorded the rotational spectral lines of the X^2B_1 electronic ground state of the H_2NS and D_2NS radicals in the 150–390 GHz region. They provided accurate equilibrium (r_e) and zero-point average structures (r_z), and estimated the 6 fundamental vibrational modes (ν_{1-6}). Theoretically, earlier works revealed the existence of four stable isomers with molecular formula H_2NS, namely H_2NS (C_{2v} symmetry), *trans*-HNSH, *cis*-HNSH and H_2SN (C_s symmetry). In 2010, Pereira et al. (2010) used the CCSD/6-311++G(d,p) technique to study the ^{1}NH + ^{2}SH → *cis*-^{2}HNSH → *trans*-^{2}HNSH → ^2H_2NS → ^{2}NS → + H_2 reactive channels. The H_2NS species are found to be intermediates in these reactions. Although this work is performed at a relatively high computational level, it does not provide structural parameters for the four H_2NS isomers with the accuracy required for their detection in the laboratory and in astrophysical surveys. In addition, it does not consider the H + HNS/HSN reactive channels, which are likely to be involved in the formation of the NS radical in the interstellar clouds, since its formation cannot be fully explained by the electron capture and following fragmentation of the protonated NS. The deduced abundances of NS differ by several orders of magnitude from the measured ones in interstellar dark clouds (Millar et al., 1991; McGonagle et al., 1994; Irvine et al., 2000). The involvement of large H-, N- and S-containing molecules is not invoked. However, these compounds may play key roles in these processes, as intermediates. In this context, H_2NS species are most likely present, as stable molecules or intermediates, in the astrophysical media mentioned and should be considered in the chemical models for the study of their physicochemical properties. Nevertheless, the main limitation of the identification of such compounds is the lack of spectroscopic data. The present work provides a set of structural, vibrational and electronic parameters for the [H,H,N,S] molecular species. It should help for their identification in astrophysical media and in the laboratory. We also show that these tetratomics undergo spin-orbit-induced predissociation and photodissociation upon absorbing UV-Vis light. These restrain the astrophysical environments where they can be formed and detected.

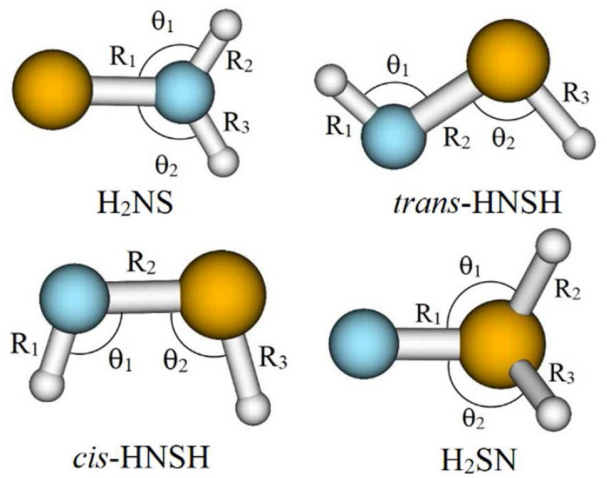

FIGURE 1 | Optimized stable forms of the H_2NS species and definition of their internal coordinates.

COMPUTATIONAL DETAILS

We started our computations by mapping the lowest doublet potential energy surface (PES) of the [H,H,N,S] molecular system to locate the stationary points (both minimal-energy and transition state structures). These geometry optimizations were done without symmetry constraints (i.e., in the C_1 point group), using the partially spin restricted coupled cluster (CC) method with a *perturbative* treatment of triple excitations [RCCSD(T)] (Hampel et al., 1992; Deegan and Knowles, 1994; Knowles et al., 2000) as well as the explicitly correlated version of this method [RCCSD(T)-F12] (Adler et al., 2007; Werner et al., 2007; Knizia and Werner, 2008; Knizia et al., 2009) and complete active space self-consistent field (CASSCF) (Knowles and Werner, 1985; Werner and Knowles, 1985) approaches as implemented in the MOLPRO suite of programs (Werner et al., 2015). The use of CC approaches is justified by the mono configurational nature of the wavefunctions of H_2NS ground state species close to equilibrium as certified by the T1 and D1 diagnostics close to 0.02 and 0.06 in Coupled Clusters computations and by the dominance of a unique configuration in their CASSCF wavefunctions (weight > 0.95). In CASSCF, the active space is formed by the whole set of valence orbitals, in which all the possible valence electron excitations are considered. For the RCCSD(T) and CASSCF computations, we used the aug-cc-pV(X+d)Z (X = D, T, Q) basis sets for sulfur and the aug-cc-pVXZ (X = D, T, Q) for hydrogen and nitrogen atoms (Kendall and Dunning, 1992; Woon and Dunning, 1993; Dunning et al., 2001). The use of tight *d* functions for sulfur improves the quality of the results, as established in the benchmark computations presented in Refs

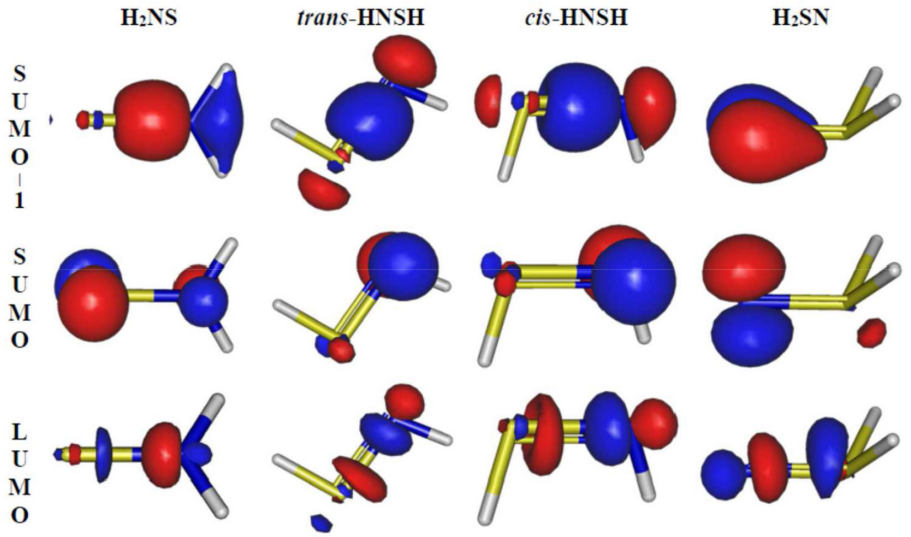

FIGURE 2 | Outermost molecular orbitals (SOMO-1, SOMO and LUMO) of the molecular species of interest obtained at the CASSCF/aug-cc-pVTZ. The isovalue is 0.13 a.u.

(BenYaghlane et al., 2013; Ben Yaghlane et al., 2014; Trabelsi et al., 2018), since it allows for a better description of the electron density of this polarizable atom and can provide accurate descriptions of the electronic structures of its compounds. In the RCCSD(T)-F12 calculations, the cc-pVXZ-F12 (X = D, T, Q) basis sets (Peterson et al., 2008) together with the corresponding auxiliary basis sets and density-fitting functions, as implemented in MOLPRO (Klopper, 2001; Weigend, 2002; Hättig, 2005), were used. These optimizations are followed by frequency computations to establish the nature of the stationary points, either minima or saddle points. Subsequently, we extrapolated the geometrical values and energetics to the CBS limit using the two-parameter equation: $A = B + C/X^3$, in conjunction with a least square procedure, where A is the extrapolated quantity, X is the cardinal number of the basis set and B and C are fitting parameters (Helgaker et al., 1997). For the RCCSD(T)/CBS and RCCSD(T)-F12/CBS geometrical parameters, we evaluated the core-valence correlation corrections at the RCCSD(T)/cc-pCVTZ and RCCSD(T)-F12/cc-pCVTZ-F12 levels, respectively. Within a given level, this was achieved by taking the difference between the optimized geometrical parameters obtained from a calculation where all the electrons are correlated and a calculation where the core electrons are kept frozen.

The PESs of the low-lying electronic states of the H_2NS species were mapped along the stretching and out-of-plane torsion coordinates with the remaining internal coordinates fixed at their respective equilibrium ground state values. These computations were carried out with the CASSCF approach followed by the internally contracted multi-reference configuration interaction (MRCI) method (Werner and Knowles, 1988; Shamasundar et al., 2011), where the H, N, and S atoms were described with the aug-cc-pV(5+d)Z basis set. In the MRCI procedure, all single and double electron excitations from the configurations of the CASSCF wavefunction having a CI coefficient larger than 0.005 were performed. The resulting MRCI wavefunctions are composed of $\sim 1.7 \times 10^7$ contracted ($\sim 1 \times 10^9$ uncontracted) configurations per C_s symmetry. Furthermore, we optimized the equilibrium geometries of the long-lived and stable electronic excited states at the CASSCF/aug-cc-pV(X+d)Z (X= T, Q, 5, CBS) level. The minimal-energy nature of these structures is indicated by all positive frequencies.

ON THE ELECTRONIC STATES OF H_2NS

For the thionitroxyl molecule, as established in the literature, our computations confirm the existence of only four stable forms in the ground state PES. Unlike H_2SN, which is located in the lowest $^2A'$ PES, H_2NS, *cis*-HNSH and *trans*-HNSH are found in the lowest $^2A''$ PES. These equilibrium structures are displayed in **Figure 1**. For each of them **Figure 2** displays the corresponding singly occupied molecular orbital (SOMO), the next-to-SOMO (SOMO-1) and the lowest unoccupied molecular orbital (LUMO) as computed at the CASSCF/aug-cc-pVTZ level. This figure shows that the SOMOs of H_2NS, *cis*-HNSH and *trans*-HNSH are π^* orbitals, while the SOMO-1s are of σ type. All these orbitals are mainly located on the NS bond. Whereas, the SOMO-1 and the SOMO of H_2SN correspond to π orbitals mainly located on the nitrogen atom. For all species, the LUMOs are σ^* SN bonds.

Figures 3–6 present one-dimensional cuts of the 6D-PESs of the doublet and quartet electronic states of H_2NS, *cis*-HNSH, *trans*-HNSH and H_2SN along the stretching coordinates, with the remaining internal coordinates kept fixed at their ground state values. We give also the evolution along the out-of-plane / torsion angle. These potentials are computed at the CASSCF/MRCI/aug-cc-pV(5+d)Z level of theory. In these cuts, energies are given with respect to the H_2NS ground state energy

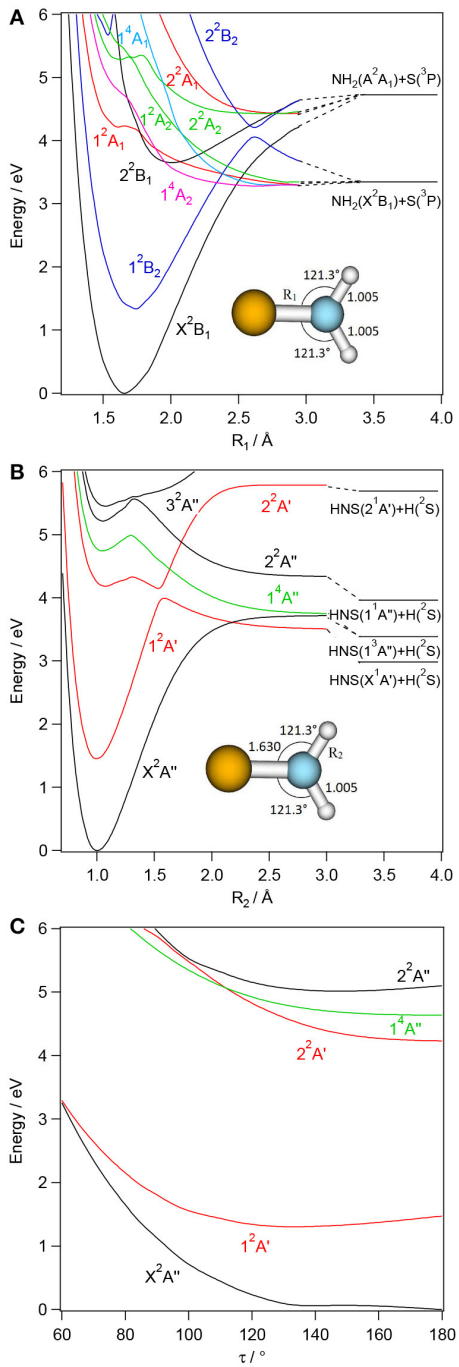

FIGURE 3 | CASSCF/MRCI/aug-cc-pV(5+d)Z one-dimensional cuts of the 6D-PESs of the low-lying electronic states of H_2NS along the NS (R_1, **A**) and NH (R_2, **B**) stretching and τ out-of-plane **(C)** coordinates. The remaining internal coordinates are kept fixed at their values in the $H_2NS(X^2B_1)$ state i.e. $R_3 = 1.630$ Å, $R_2 = R_3 = 1.005$ Å, $\theta_1 = \theta_2 = 121.3°$ and $\tau = 180°$ (for planar configuration). The H + HNS/HSN and NH_2 + S asymptotes are located using the data in **Supplementary Tables 8**, **9** and (Xin et al., 2003; Trabelsi et al., 2015)[1].

at equilibrium. These potentials correlate adiabatically to the HNS/HSN + H or NH + HS or NH_2 + S or H_2S + N dissociation limits at internuclear separations. **Table 1** lists the electronic states of H_2NS species located in the 0–6.5 eV internal energy range and gives also their CASSCF/MRCI/aug-cc-pV(5+d)Z vertical electronic excitation energies and dominant electronic configurations, as quoted at the equilibrium geometry of the corresponding electronic state.

For each [H,H,N,S] isomer, **Figures 3–6** reveal that the two lowest electronic states have deep potential wells along the stretching coordinates. Besides, the ground electronic states are well-separated from the upper ones in the molecular region and free from interactions that could lead to mixing of their wavefunctions. Therefore, these electronic states are monoconfigurational in nature and can be accurately described by the monoconfigurational post-Hartree-Fock methods used in the present investigation (cf. *infra*).

Table 1 shows that the first excited states are obtained upon SOMO-1 → SOMO electron promotion. In the Franck-Condon region accessed from the corresponding ground states, the first excited states correspond to 1^2B_2, $1^2A'$, $1^2A'$, and $1^2A''$ space symmetry species for H_2NS, *cis*-HNSH, *trans*-HNSH, and H_2SN, respectively. They are located at 1.15 – 1.5 eV for $H_2NS(1^2B_2)$ and $H_2SN(1^2A'')$ and at 3–3.4 eV for *cis*-HNSH($1^2A'$) and *trans*-HNSH($1^2A'$) with respect to their corresponding electronic ground state. At equilibrium, they possess non-planar configurations with C_s symmetry for H_2NS and H_2SN and C_1 symmetry for HNSH. For *cis*-HNSH and *trans*-HNSH a unique minimum is found in the 2^2A state PES, whereas both *cis* and *trans* forms exist in the ground state potential. Moreover, the lowest electronic excited states interact with the other states for non-planar configurations. For instance, **Figure 4** shows that the local minimum in the HNSH excited PES is due to an avoided crossing between the lowest doublets at $\tau \sim 100°$. In this region the wavefunctions of both states are mixed and acquire multiconfigurational character. Such states should be investigated using multi configurational approaches (cf. infra).

For the low-lying doublet excited states of **Table 1**, we calculated the oscillator strengths from the vertical excitation energies and transition moments evaluated at the CASSCF/MRCI/aug-cc-pV(5+d)Z level. The calculated values show that rather intense transitions are expected from the X^2B_1 to the 2^2B_1 state of H_2NS and from the ground to the $2^2A''$ states of *trans*-HNSH, *cis*- HNSH and H_2SN. The other transitions range from very weak to moderately weak.

In the Franck-Condon region accessed from the corresponding electronic ground states, the upper electronic states of H_2NS, *trans*-HNSH, *cis*- HNSH and H_2SN are located above 4 eV. They correspond to electron excitations from the occupied inner valence MOs to the LUMO and LUMO+1 unoccupied MOs. The shapes of the resulting potentials are far from the standard Morse-like ones, since most of them are repulsive at large distances. Local minima can also exist at short distances and for non-planar configurations. Moreover, there is a high density of electronic states, which favors the mixing of their wavefunctions by vibronic and spin-orbit couplings. For instance, the quartets are crossing the doublets at intermediate R distances where spin-orbit conversion may occur. At these distances, the quartets are mostly repulsive and lead to fragmentations. For instance, the lowest quartet is crossing

[1]https://webbook.nist.gov

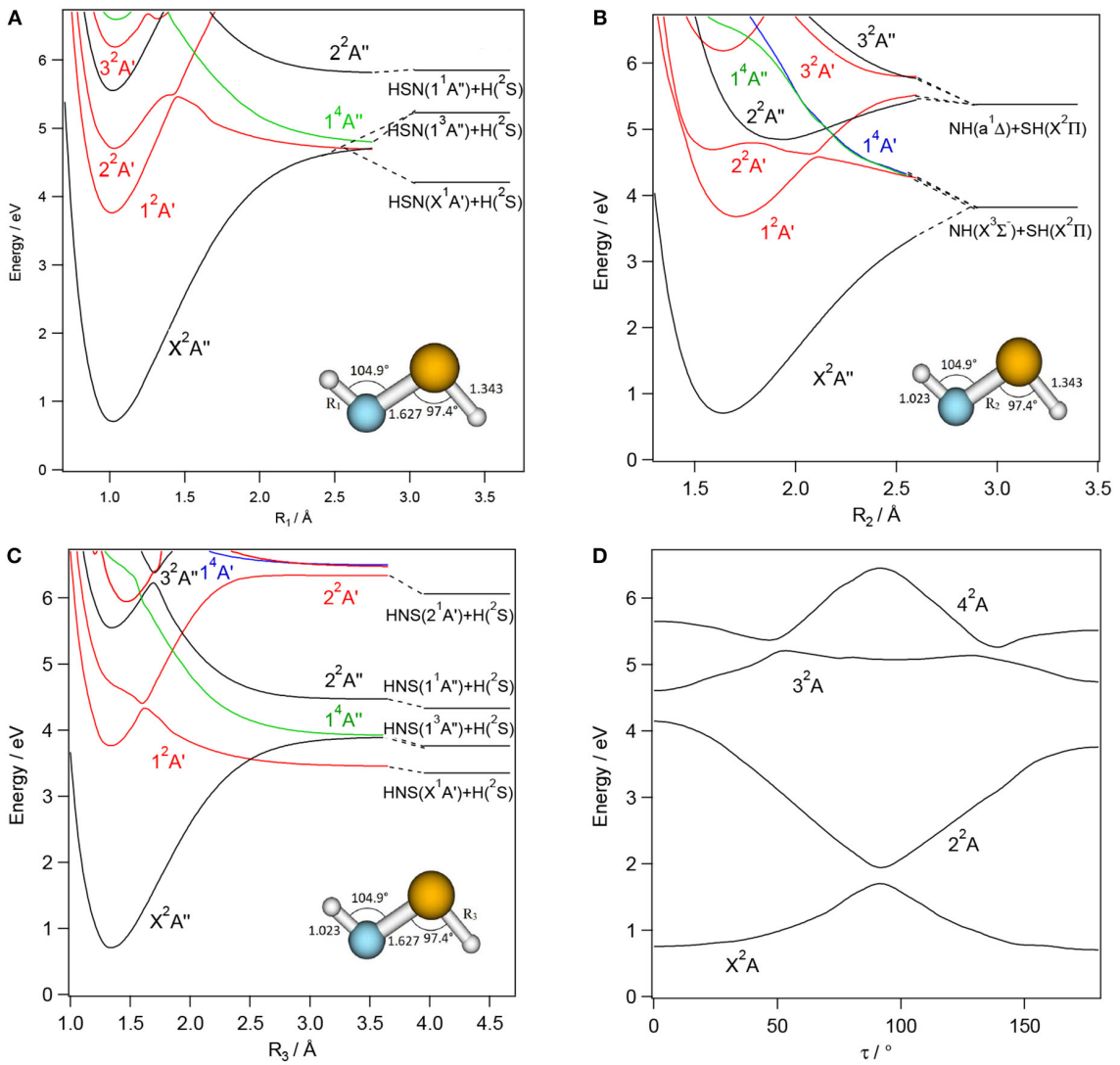

FIGURE 4 | CASSCF/MRCI/aug-cc-pV(5+d)Z one-dimensional cuts of the 6D-PESs of the low lying electronic states of *trans*-HNSH along the SH (R_1, **A**), NS (R_2, **B**), and NH (R_3, **C**) stretching and τ torsion, **(D)** coordinates. The remaining internal coordinates are kept fixed at their values in the *trans*-HNSH(X^2A'') state i.e., R_1 = 1.023 Å, R_2 = 1.627 Å, R_3 = 1.343 Å, θ_1 = 104.9° θ_2 = 97.4°, and τ = 180°. The H + HNS/HSN, NH + SH asymptotes are located using the data in **Supplementary Tables 8**, **9** and (Trabelsi et al., 2015)[1]. The reference energy is that of $H_2NS(X^2B_1)$ at equilibrium.

the electronic excited doublets at different nuclear geometries, where spin-orbit-induced predissociations may happen. At large internuclear separations, the reactions evolve along the repulsive part of this quartet state, which correlates adiabatically to lower dissociation limits. This is the case indeed for H_2NS, where a crossing between the $H_2NS(2^2A')$ and the $H_2NS(1^4A'')$ states occurs at NH ∼1.6 Å (**Figure 3**). For this doublet, we note also an avoided crossing with the $1^2A'$ state at NH ∼1.5 Å (**Figure 3**), where vibronic coupling may occur. Interestingly this avoided crossing is responsible for the double well-shape of $H_2NS(2^2A')$ and *cis*-HNSH($2^2A'$) along the SN distance. Also, the cuts of the PESs show that the second electronic excited state presents a flat potential along the torsion/out-of-plane coordinate resulting in a planar structure for H_2NS, whereas two minima can be seen for HNSH (*cis* and *trans*) and for H_2SN (C_{2v} and C_s). In all cuts displayed in **Figures 3–6**, the potential of such state has generally an odd shape, which may favor intramolecular isomerizations converting H_2NS into HNSH and H_2SN, and *vice versa*.

STRUCTURE AND SPECTROSCOPY OF LOWEST ELECTRONIC STATES OF THE H_2NS SPECIES

For the investigation of the structure and vibrational spectroscopy of [H,H,N,S] in their electronic ground states, we used monoconfigurational approaches since their electronic

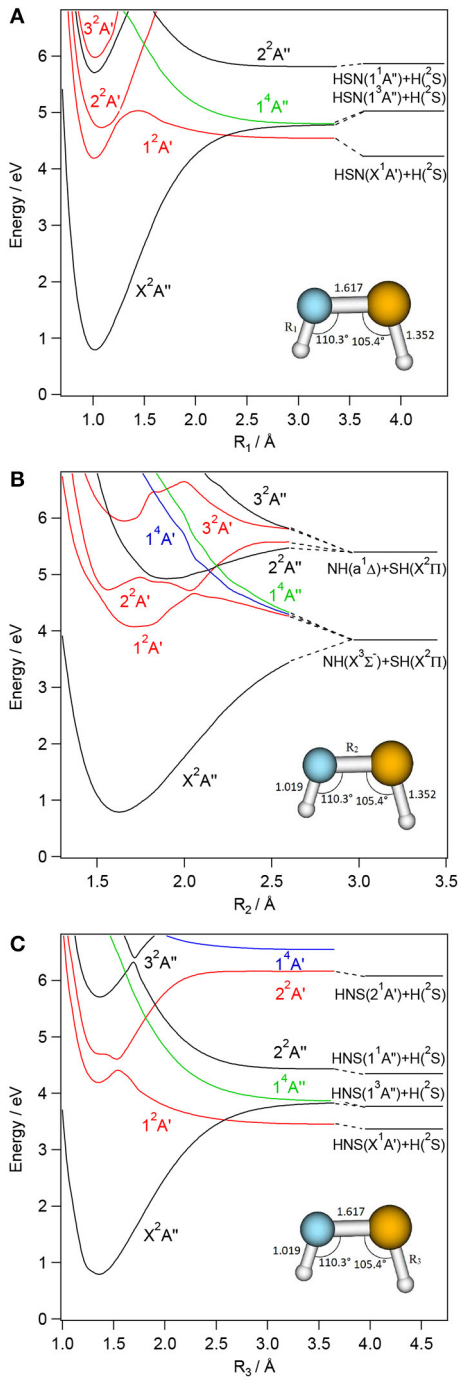

FIGURE 5 | CASSCF/MRCI/aug-cc-pV(5+d)Z one-dimensional cuts of the 6D-PESs of the low lying electronic states of *cis*-HNSH along the SH (R_1, **A**), NS (R_2, **B**) and NH (R_3, **C**) stretching coordinates. The remaining internal coordinates are kept fixed at their values in the *cis*-HNSH(X^2A'') state i.e., $R_1 = 1.019$ Å, $R_2 = 1.617$ Å; $R_3 = 1.352$ Å, $\theta_1 = 110.3°$, $\theta_2 = 105.4°$, and $\tau = 0°$. The H + HNS/HSN, NH + SH asymptotes are located using the data in **Supplementary Tables 8**, **9** and (Trabelsi et al., 2015)[1]. The reference energy is that of $H_2NS(X^2B_1)$ at equilibrium.

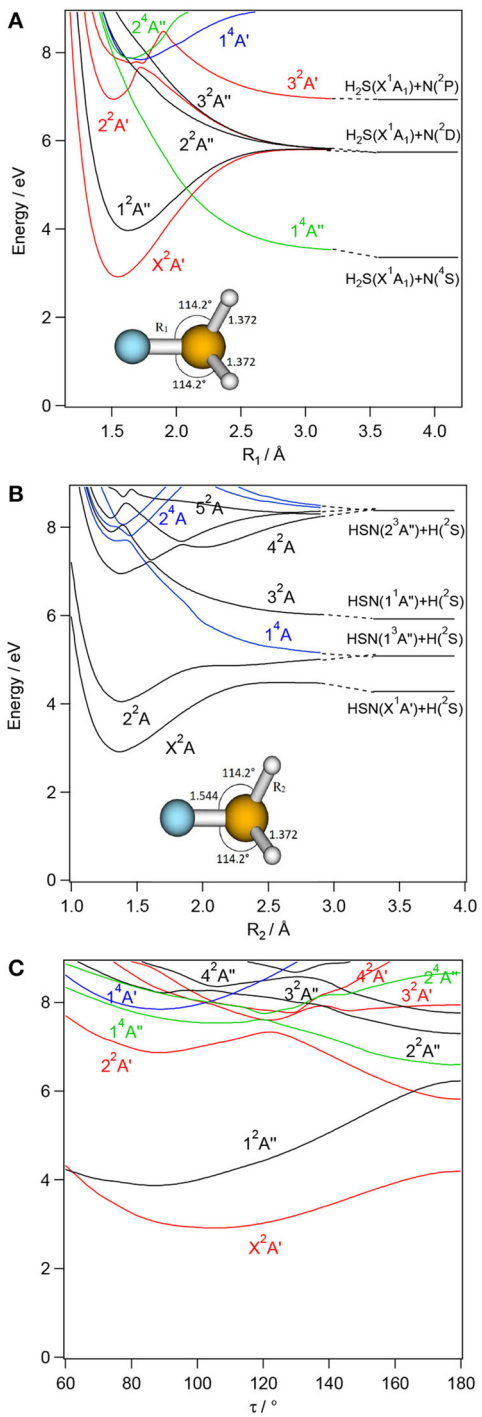

FIGURE 6 | CASSCF/MRCI/aug-cc-pV(5+d)Z one dimensional cuts of the 6D-PESs of the low lying electronic states of H_2SN along the NS (R_1, **A**) and NH (R_2, **B**) stretching coordinates and τ torsion, **(C)** coordinate. The remaining internal coordinates are kept fixed at their values in the $H_2SN(X^2A')$ state i.e., $R_1 = 1.544$ Å, $R_2 = R_3 = 1.372$ Å, $\theta_1 = \theta_2 = 114.2°$, and $\tau = 104.1°$. The H + HNS/HSN and H_2S + N asymptotes are located using the data in **Supplementary Tables 6**, **7** and (Trabelsi et al., 2015)[1]. The reference energy is that of $H_2NS(X^2B_1)$ at equilibrium.

wavefunctions, as discussed above, can be dominantly described by a unique configuration close to equilibrium. Thus, we characterized the stable forms of this molecular system in the ground state PES at the RCCSD(T)/aug-cc-pV(X+d)Z (X=D, T, Q) and RCCSD(T)-F12/cc-pVXZ-F12 (X=D, T, Q) levels of theory. **Supplementary Tables 1–4** report the corresponding optimized geometrical parameters, harmonic frequencies and total energies for the minimal structures and **Supplementary Table 5** those of the transition states. These tables show that the computed bond distances present slight variations by increasing the size of the basis set, where a systematic shortening of the bond distances is noticed because of the refined description of the electron correlation with the larger basis sets. Besides, variations in the bond angles are almost negligible upon changing the basis set.

We give in **Table 2** the data after CBS extrapolation, together with their comparison to previous works. Computations confirm the existence of the already predicted H_2NS, *trans*-HNSH, *cis*-HNSH, and H_2SN forms and the transition states connecting them. The nature of these stationary points was carefully checked by harmonic frequency analysis, as given in **Supplementary Tables 1–5**. No other isomers were located. The relative energies confirm the previously established order: H_2NS followed by *trans*-HNSH, *cis*-HNSH and H_2SN. **Table 2** shows also that all these compounds have relatively large dipole moments ($1.1 < \mu_e < 3.7$ debye). Therefore, these molecular species are susceptible to be observed by high-resolution rotational spectroscopy techniques in the laboratory and by radioastronomy. To-date, only H_2NS (X^2B_1) was identified by Habara et al. (1998) using a source-modulation microwave spectrometer and a Fourier-transform microwave spectrometer. These authors deduced an accurate equilibrium molecular structure: $R_{NS} = R_1 = 1.6398$ Å, $R_{NH} = R_3 = R_2 = 1.0055$ Å and in-plane angle $\theta_1 = \theta_2 = 120.5°$. Our RCCSD(T)/CBS and RCCSD(T)-F12/CBS values compare well with this experimental geometry, with deviations of less than 0.6%. As expected, the less accurate previous calculations lead to larger deviations. For the other not yet detected isomers, we expect a similar accuracy. From the RCCSD(T)/CBS and RCCSD(T)-F12/CBS optimized geometries, we deduced the equilibrium rotational constants (A_e, B_e, C_e), to which we added the respective vibrational and centrifugal distortion corrections computed at the RMP2/aug-cc-pV(Q+d)Z level, within the VPT2 approach. Hence, at the RCCSD(T)/CBS level, the corrected (A_0, B_0, C_0) rotational constants of **Table 2** are straightforwardly obtained from the following equation:

B_0(RCCSD(T)/CBS) = B_e(RCCSD(T)/CBS) + B_0(RMP2/aug-cc-pV(Q+d)Z) – B_e(RMP2/aug-cc-pV(Q+d)Z)

and similarly for A_0(RCCSD(T)/CBS), C_0(RCCSD(T)/CBS), A_0(RCCSD(T)-F12/CBS), B_0(RCCSD(T)-F12/CBS), and C_0(RCCSD(T)-F12/CBS). **Table 2** shows that we have good agreement with the experimental data by Habara et al. (1998).

Table 2 lists the anharmonic frequencies of the fundamental modes (ν_i), which have been evaluated using the RCCSD(T)/aug-cc-pV(Q+d)Z//RMP2/aug-cc-pV(Q+d)Z composite scheme described in Hochlaf et al., 2015). Here, ν_i is equal to $\omega_i + \Delta\nu_i$, where ω_i is the RCCSD(T)/aug-cc-pV(Q+d)Z

TABLE 1 | Dominant electronic configurations of the lowest-lying electronic states of H_2NS, *cis*- and *trans*-HNSH and H_2SN at the corresponding ground state equilibrium geometry.

State	T_v	Electronic configuration	*f*	State	T_v	Electronic configuration	*f*	State	T_v	Electronic configuration	*f*	State	T_v	Electronic configuration	*f*
		H_2NS				*trans*-HNSH				*cis*-HNSH				H_2SN	
X^2B_1	0.0	$(2b_1)^2(3b_2)^2(3b_1)^1$		X^2A''	0.0	$(2a'')^2(10a')^2(3a'')^1$		X^2A''	0.0	$(2a'')^2(10a')^2(3a'')^1$		X^2A'	0.0	$(9a')^2(3a'')^2(10a')^1$	
1^2B_2	1.44	$(2b_1)^2(3b_2)^1(3b_1)^2$		$1^2A'$	3.05	$(2a'')^2(10a')^1(3a'')^2$	0.00127	$1^2A'$	3.40	$(2a'')^2(10a')^1(3a'')^2$	0.00561	$1^2A''$	1.14	$(9a')^2(3a'')^1(10a')^2$	0.00099
1^2A_1	4.23	$(2b_1)^2(3b_2)^2(8a_1)^1$	0.00023	$2^2A'$	4.00	$(2a'')^2(10a')^2(11a')^1$	0.00002	$2^2A'$	3.99	$(2a'')^2(10a')^2(11a')^1$	0.00066	$2^2A'$	4.05	$(9a')^1(3a'')^2(10a')^2$	0.00209
1^4A_2	4.75	$(2b_1)^2(3b_2)^1(3b_1)^1(8a_1)^1$		$2^2A''$	4.84	$(2a'')^2(10a')^1(3a'')^1(11a')^1$	0.02442	$2^2A''$	4.91	$(2a'')^1(10a')^2(3a'')^2$	0.04559	$1^4A''$	4.76	$(9a')^2(3a'')^1(10a')^1(12a')^1$	
2^2B_1	4.92	$(2b_1)^1(3b_2)^2(3b_1)^2$	0.10533	$3^2A'$	5.48	$(2a'')^2(10a')^2(12a')^1$	0.00161	$3^2A'$	5.18	$(2a'')^2(10a')^2(12a')^1$	0.00116	$3^2A'$	4.94	$(9a')^2(3a'')^2(11a')^1$	0.00089
1^2A_2	5.29	$(2b_1)^2(3b_2)^1(3b_1)^1(8a_1)^1$	0.00230	$1^4A''$	5.89	$(2a'')^2(10a')^1(3a'')^1(13a')^1$		$1^4A''$	6.43	$(2a'')^2(10a')^1(3a'')^1(12a')^1$		$2^4A''$	5.08	$(9a')^2(3a'')^1(10a')^1(11a')^1$	
2^2A_2	5.46	$(2b_1)^2(3b_2)^1(3b_1)^1(8a_1)^1$	0.00071									$1^4A'$	5.16	$(9a')^2(3a'')^1(10a')^1(4a'')^1$	
												$2^2A''$	5.23	$(9a')^2(3a'')^1(10a')^1(11a')^1$	0.01455
												$3^2A''$	5.93	$(9a')^2(3a'')^1(10a')^1(11a')^1$	0.00409

We also give the vertical excitation energy T_v (in eV) as computed at the CASSCF/MRCI/aug-cc-pV(5+d)Z level. T_v is given with respect to the corresponding ground state energy at equilibrium. Oscillator strengths f for electronic excitations from the ground state are obtained from the vertical excitation energies and transition moments evaluated at the CASSCF/MRCI/aug-cc-pV(5+d)Z level.

harmonic frequency of the i-th mode, and $\Delta\nu_i$ is the corresponding RMP2/aug-cc-pV(Q+d)Z anharmonic correction (**Supplementary Table 6**) as determined using second-order vibrational perturbation theory (VPT2) (Mills, 1972; Aliev and Watson, 1985), as implemented in GAUSSIAN. The validity of such procedure was widely discussed in (Carbonnière et al., 2005; McKean et al., 2008; Temelso and Shields, 2011; Zen et al., 2012). Briefly, it allows to predict accurate and fully *ab initio* anharmonic vibrational frequencies at a low computational cost.

For $H_2NS(X^2B_1)$, we compute ν_1 = 3400.5, ν_2 = 1566.2, ν_3 = 938.9, ν_4 = 3503.5, ν_5 = 1015.4 and ν_6 = 412.9 (all values in cm^{-1}). These fundamentals are of a_1 symmetry for ν_1-ν_3, b_2 symmetry for ν_4-ν_5 and b_1 symmetry for ν_6 (out-of-plane mode). They compare favorably with the values by Habara et al. (1998) for the following modes: ν_1 (= 3430 cm^{-1}), ν_3 (= 918 cm^{-1}), ν_4 (= 3553 cm^{-1}) and ν_5 (= 989 cm^{-1}), while the comparison is less satisfactory for ν_2 (= 1328 cm^{-1}) and ν_6 (= 325 cm^{-1}). Also, we found that the ν_6 mode is strongly anharmonic, with inverted anharmonicity. This is related to the flatness of the PES along this normal coordinate. VPT2 treatment is not enough for deducing the ν_6 frequency. Instead, a full variational treatment in a 6D-PES is needed, which is beyond the scope of the present work.

For *cis*-HNSH and *trans*-HNSH, ν_1 through ν_5 are of a' symmetry, and ν_6 is of a'' symmetry, while for H_2SN ν_1 through ν_4 are of a' symmetry, and ν_5 and ν_6 are of a'' symmetry. **Table 2** lists their fundamentals. Moreover, **Table 2** lists the respective IR intensities, which show that all the possible modes are potentially detectable in the IR spectra.

Supplementary Figure 1 and **Supplementary Table 5** give the optimized transition states (TS_1-TS_4) geometries, harmonic frequencies and total energies as calculated at the RCCSD(T)/aug-cc-pV(X+d)Z and RCCSD(T)-F12/cc-pVXZ (X=D,T,Q, CBS) levels. TS_1 connects *cis*-HNSH and *trans*-HNSH. The corresponding isomerization barrier is computed to be 0.88 eV at the RCCSD(T)/CBS level. TS_2 connects *trans*-HNSH and H_2NS. It is located at 1.84 eV above *trans*-HNSH. TS_3 and TS_4 are transition states along the H_2NS and H_2SN $\rightarrow$ H_2 + NS production channels, respectively. The energy barrier for $H_2NS \rightarrow TS_3$ is relatively large (> 3 eV) and that of $H_2SN \rightarrow H_2$ + NS is about 1 eV. The relative energies and the structures of these transition states are close and consistent with the data obtained by Pereira et al. (2010) using the CCSD/6-311++G(d,p) approach. The interconversion processes through these transition states may compete with the photophysical processes discussed in Section Photochemistry.

Table 3 lists the CASSCF/CBS optimized geometrical and spectroscopic parameters of the first electronic excited state for each isomer. The full set of data is given in **Supplementary Table 7**. Here, only three structures are found since *cis*- and *trans*-HNSH have the same excited state for non-planar HNSH arrangement. The comparison of the bond distances in $H_2NS(X^2B_1)$ and $H_2NS(1^2A')$ reveals that the SN distance is lengthened upon electronic excitation, since the outermost electron is promoted from a bonding MO (SOMO-1) to an antibonding MO (SOMO), as illustrated in **Figure 2**. On the contrary, the NH bonds are only slightly affected. This is also the case for H_2SN, whereas no variations are seen for the HNSH species.

For the calculated electronic state of each isomer, we evaluated the radiative lifetime (τ_{rad}) using the formula

$1/\tau_{rad} = \Sigma_i\ 1/\tau_{i,rad}$, where $\tau_{i,rad}$ (= 6.07706 /($|R_{e,i}|^2$ $(\Delta E_{a,i})^3$) in μs) is the radiative lifetime populating the lower doublet states. Here, $|R_{e,i}|$ (in debye) is the transition moment between the upper and the lower states as computed at the CASSCF/aug-cc-pV(5+d)Z level, and $\Delta E_{a,i}$ (in eV) is the corresponding CASSCF/MRCI/aug-cc-pV(5+d)Z adiabatic excitation energy.

Radiative lifetime computations were carried out at the ground state ($\tau_{rad,g}$) and excited state ($\tau_{rad,e}$) equilibrium geometries. The results are summarized in **Table 3**. This table shows that the calculated lifetimes are at least of several hundred ns, i.e., long enough to allow these electronic states to emit if populated.

PHOTOCHEMISTRY

In order, to understand the thermodynamic aspects of the different dissociation processes taking place in [H,H,N,S] species or their formation from simple fragments, we give in **Figure 7** the fragmentation energies to form diatomic + diatomic and atomic + triatomic entities, which are computed using:

$$E_0 = E(AB) + E(CD) - E(ABCD) + ZPE(AB) + ZPE(CD) - ZPE(ABCD).$$

or

$$E_0 = E(ABC) + E(D) - E(ABCD) + ZPE(ABC) - ZPE(ABCD).$$

where E(D), E(AB), E(CD), E(ABC) and E(ABCD) are the total energies of the D, AB, CD, ABC and ABCD entities. The ZPEs are their zero-point vibrational energies.

Figure 7 shows that the electronic ground state of each isomer is located below the lowest dissociation limit, i.e., $HNS(X^2A')$+$H(^2S)$. Therefore, all the calculated species are expected to be stable with respect to dissociation. All bimolecular reactions may lead to their formation. This is also the case for the first excited states of H_2NS and HNSH (denoted as H_2NS^* and HNSH* in **Figure 7**). Such compounds are also expected to be long-lived. **Table 3**, which gives their radiative lifetimes, confirm such assumptions. Indeed, we compute lifetimes of several hundreds of ns for H_2NS^* and HNSH*. On the other hand, the lifetime of the first electronic excited state of H_2SN (labeled H_2SN^*) may be reduced by spin-orbit-induced predissociation to populate the SN bond breaking channels $HNS(X^2A')$+$H(^2S)$, $NH_2(X^2B_1)$+$S(^3P)$ or $H_2S(X^1A_1)$+$N(^4S)$. **Figure 6** shows that the latter process is plausible since the $H_2SN^*(1^2A'')$ is crossed by the repulsive $1^4A''$ state which leads directly to these fragments. **Figure 7** shows also that the second electronic excited states of all species are located above the lowest dissociation limit. Their lifetimes should be reduced by predissociation phenomena via the couplings with the quartet manifolds. Nevertheless, **Table 3** shows that

TABLE 2 | Optimized equilibrium geometries and relative energies (E_r, eV) of [H,H,N,S] isomers as computed at the RCCSD(T)/CBS and CCSD(T)-F12/CBS levels of theory.

Struct.	Method	R_1	R_2	R_3	θ_1	θ_2	τ	E_r	μ_e	ν_1	ν_2	ν_3	ν_4	ν_5	ν_6	A_O	B_O	C_O
H_2NS (X^2B_1) C_{2v}	Calc.[a]	1.635 (1.637)	1.005 (1.006)	1.005 (1.006)	121.3 (121.3)	121.3 (121.3)	180 (180)	0	2.52	3400.5 (29)	1566.2 (8)	938.9 (14)	3503.5 (62)	1015.4 (9)	412.9[h] (122)	332.5581	16.0118	15.2798
	Calc.[b]	1.627 (1.630)	1.004 (1.005)	1.004 (1.005)	121.3 (121.3)	121.3 (121.3)	180 (180)	0	2.55							333.2358	16.1639	15.4198
	Exp.[c]	1.6398	1.0055	1.0055	120.5	120.5	-	-	-	3430[g]	1328[g]	918[g]	3553[g]	989[g]	325[g]	333.451 (139)	16.12137 (27)	15.37089 (27)
	Calc.	1.641[d] 1.644[f]	1.008[d]	1.008[d]	121.4[d]	121.4[d]		0[d]		3430[d] 3610[f]	1560[d] 1652[f]	918[d] 951[f]	3553[d] 3730[f]	1001[d] 1059[f]	259[d] 189[f]			
trans-HNSH (X^2A'') C_s	Calc.[a]	1.020 (1.021)	1.623 (1.627)	1.339 (1.341)	104.9 (104.8)	97.4 (97.4)	180 (180)	0.706	1.11	3280.1 (10)	2558.4 (0.4)	1206.1 (28)	961.3 (26)	812.0 (13)	624.2 (60)	196.8256	17.7622	16.2608
	Calc.[b]	1.022 (1.023)	1.623 (1.627)	1.341 (1.343)	105.0 (104.9)	97.4 (97.4)	180 (180)	0.697	1.11							196.2710	17.7573	16.2529
	Calc.	1.023[d] 1.063[e]	1.639[d] 1.750[e] 1.661[d]	1.336[d] 1.350[e]	104.5[d] 114.4[e]	96.9[d] 103.1[e]		0.766[d]		3462[f]	2737[f]	1249[f]	983[f]	813[f]	633[f]			
cis-HNSH (X^2A'') C_s	Calc.[a]	1.016 (1.017)	1.614 (1.618)	1.348 (1.350)	110.4 (110.2)	105.3 (105.3)	0 (0)	0.791	2.34	3322.4 (7)	2477.7 (12)	1129.8 (26)	953.4 (20)	785.0 (0.5)	540.3 (24)	200.9696	17.7559	16.2853
	Calc.[b]	1.018 (1.019)	1.613 (1.617)	1.350 (1.352)	110.4 (110.3)	105.4 (105.4)	0 (0)	0.781	2.36							200.4284	17.7731	16.2961
	Calc.	1.020[d]	1.629[d] 1.653[d]	1.347[d]	110.2[d]	104.4[d]	-	0.853[d]	-	3496[f]	2651[f]	1178[f]	972[f]	791[f]	467[f]			
H_2SN (X^2A') C_s	Calc.[a]	1.542 (1.545)	1.367 (1.369)	1.367 (1.369)	114.1 (114.1)	114.1 (114.1)	103.9 (103.9)	2.916	3.71	2256.3 (104)	1275.5 (38)	965.4 (12)	772.2 (0.3)	2224.5 (76)	789.3 (8)	167.2792	19.1039	18.4406
	Calc.[b]	1.541 (1.544)	1.370 (1.372)	1.370 (1.372)	114.2 (114.2)	114.2 (114.2)	104.1 (104.1)	2.904	3.70							166.8030	19.1182	18.4450
	Calc.	1.567[d] 1.574[f]	1.369[d]	1.369[d]	114.1[d]	114.1[d]	103.4[d]	2.997[d]	-	2441[f]	1342[f]	928[f]	801[f]	2386[f]	822[f]			

μ_e (Debye) is the dipole moment at equilibrium. Distances are in Å and angles are in degrees. We give the anharmonic frequencies (ν_i, in cm^{-1}) as deduced using the RCCSD(T)/aug-cc-pV(Q+d)Z//RMP2/aug-cc-pV(Q+d)Z composite scheme. In parentheses, we give their IR intensities (in km mol^{-1}). In addition, we give the rotational constants (in GHz), evaluated at the RCCSD(T)/CBS and RCCSD(T)-F12/CBS levels, including vibrational and centrifugal distortion corrections (see the text for more details).

[a] This work, RCCSD(T)/CBS level. Geometrical parameters are corrected for core-valence correlation effects, computed at the RCCSD(T)/cc-pCVTZ level, as detailed in the text (the RCCSD(T)/CBS values are given in parenthesis).

[b] This work, RCCSD(T)-F12/CBS level. Geometrical parameters are corrected for core-valence correlation effects, computed at the RCCSD(T)-F12/cc-pCVTZ-F12 level, as detailed in the text (the RCCSD(T)-F12/CBS values are given in parenthesis).

[c] Microwave spectrum (Habara et al., 1998).

[d] Harmonic frequencies as computed at the MP2/6311++G(d,p) level of theory (Nguyen et al., 1994).

[e] Harmonic frequencies as computed at the Double-zeta basis set using the Gaussian 70 program (Miura et al., 1983).

[f] Harmonic frequencies as computed at the CCSD/6-311++G(d,p) level of theory (Pereira et al., 2010).

[g] Estimation from the Microwave spectrum (Habara et al., 1998).

[h] Strongly anharmonic. See text.

TABLE 3 | CASSCF/CBS optimized equilibrium geometries of [H,H,N,S] isomers in their lowest electronic excited states.

	R_1	R_2	R_3	θ_1	θ_2	τ	ΔE_a^a	ΔE_e^a	$\tau_{rad,g}$	$\tau_{rad,e}$
$H_2NS(1^2A')$	1.782	1.029	1.029	103.9	103.9	106.0	0.884	0.543	-[d]	577447
$HNSH(2^2A)$	1.012	1.661	1.357	114.4	103.8	90.9	1.171[b]	0.237	1.8[b]	2026
							1.147[c]		0.38[c]	
$H_2SN(1^2A'')$	1.627	1.365	1.365	106.8	106.8	91.8	0.869	0.685	18.28	156.05
$H_2NS(2^2A')$	2.128	1.030	1.030	115.6	115.6	128.5	3.795	2.073	0.006	0.33
cis-$HNSH(2^2A')$	1.035	1.643	1.491	116.9	88.0	0.0	3.424[c]	2.862	0.57[b]	2.24
									0.14[c]	
$H_2SN(2^2A')$	1.511	1.380	1.380	110.3	110.3	93.6	3.867	3.768	0.45	0.46

Distances are in Å and angles are in degrees. We give also the adiabatic transition energies (ΔE_a, eV) as computed at the CASSCF/MRCI/aug-cc-pV(5+d)Z level with respect to the corresponding electronic ground state. ΔE_e (in eV) is the energy difference between the excited state and the ground state at the equilibrium geometry of the excited state. $\tau_{rad,g}$ and $\tau_{rad,e}$ (in μs) are the radiative lifetimes at equilibrium of the ground and electronic excited states, respectively. See ***Figure 1*** *for the definition of the internal coordinates. The harmonic frequencies are given in* ***Supplementary Table 7****.*

[a] *CASSCF/MRCI/aug-cc-pV(5+d)Z computations.*

[b] *With respect to trans-HNSH(X^2A'').*

[c] *With respect to cis-HNSH(X^2A'').*

[d] *Forbidden transition.*

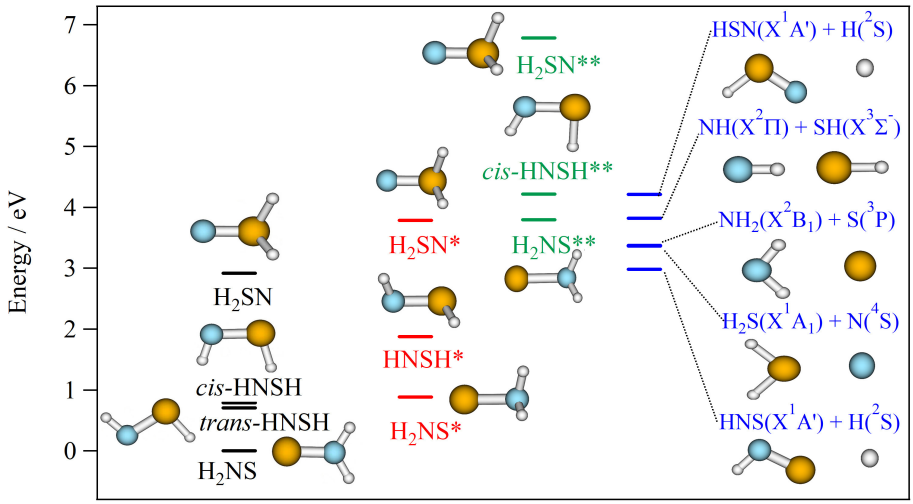

FIGURE 7 | (R)CCSD(T)/CBS fragmentation energies (in eV) of H_2NS, *trans*-HNSH, *cis*- HNSH and H_2SN forming HNS/HSN + H; NH_2 + S, H_2S + N and NH_2 + SH. These energies are given with respect to the H_2NS ground state at equilibrium. Molecular species denoted by * and ** are electronically excited species in the first and second excited states, respectively (**Table 3**). All molecular species are taken at their equilibrium structure as optimized at the respective theoretical level. The ZPE correction is also included. See **Supplementary Tables 8**, **9** for more details.

their radiative lifetimes are long enough to fluoresce whenever populated. For the upper electronic states (> 4 eV), they are located in energy above the lowest dissociation limit. They may undergo unimolecular decomposition processes forming H+HNS/HNS, H_2+NS or NH+SH. A multi-step mechanism along the PESs of their doublet states is expected, where the wavepackets on these PESs evolve until reaching the regions of conical intersections or avoided crossings. The electronic de-excitation of the H_2NS, *trans*-HNSH, *cis*- HNSH and H_2SN molecules may occur via emission of light or more likely by radiationless internal conversion processes. The lowest states are thus populated. Alternatively, a conversion to the quartet manifold takes place at the doublet-quartet crossings, followed by dissociation.

In their pioneering work on "active nitrogen," Strutt, Fowler and Vaidya (Strutt and Fowler, 1912; Strutt, 1913; Fowler and Vaidya, 1931) and later on Westbury and Winkler (Westbury and Winkler, 1960) showed that the reactions of "active nitrogen" with hydrogen sulfide occurring in a flame are associated with a deep blue glow that appeared to fill the entire upper half of the reaction vessel. This light emission was interpreted as emanating from the N.H_2S tetratomic intermediate. Computations show that the bimolecular reactive collisions, in the presence of a third party to absorb the excess energy, should lead to the formation of [H,H,N,S] tetratomics in their electronic ground states as established by Pereira et al. (2010) for the ^1NH + ^2SH → *cis*-^2HNSH → *trans*-^2HNSH → ^2H_2NS → ^2NS + H_2 reactive channels. Also the [H,H,N,S] tetratomics can be

formed in their first electronic excited states, which are long-lived enough to emit light in the IR domain ($h\nu < 1.2$ eV, **Table 3**). Nevertheless, such light was not observed in the experiment most likely because it was not possible to measure it at the beginning of the XXth century. **Table 3** shows also that the second electronic excited state of [H,H,N,S] species can be a suitable candidate to explain the deep blue glow. Indeed the $H_2SN(X^2A') \leftarrow H_2SN(2^2A')$ transition has an energy of ∼3.8 eV. As mentioned above the PES of this electronic state is flat, so intramolecular isomerization to form the other isomers is possible. At least, we may obtain the *cis*-HNSH ($2^2A'$) species, which is long lived enough to emit light with $h\nu \sim 2.8$ eV i.e., close to the ∼2.7 eV experimentally observed deep blue glow. Thus, our work establishes that the less stable forms HSNH and H_2SN are responsible for the flame color. **Figure 6** shows that the upper state can be populated after collisions between $N(^2D)$ or $N(^2P)$ with H_2S, which means that the N atom is not in its electronic ground state (^4S). Accordingly, the so-called "active nitrogen" corresponds to electronically excited nitrogen atoms that might be formed in the flame. The reactions evolve on the PESs of the electronic excited states of doublet spin multiplicity.

CONCLUSIONS

Using advanced *ab initio* methodologies, we mapped the PESs of the lowest electronic states of the [H,H,N,S] molecular species. Thence, we characterized the stable forms in the ground and two lowest electronic states. For the ground states, we confirm the existence of the four already known isomers. Since the corresponding experimental data are estimates, we suggest that the IR spectra of these compounds should be measured again for a definitive conclusion. On the excited potentials, the H_2NS, HNSH and H_2SN forms were identified for the first time. Also, we used these potentials to examine the unimolecular decomposition processes undergone by the H_2NS, HNSH and H_2SN species and the bimolecular reactions processes between H and HNS/HSN, NH + SH and H_2S + N. The findings relative to the latter process were used to confirm the observation of H_2SN fluorescent as an intermediate during the reactions between "active nitrogen" and H_2S, known since the beginning of the XXth century. Our data should help in identifying [H,H,N,S] molecular compounds in the laboratory as well as in astrophysical and environmental media.

DATA AVAILABILITY STATEMENT

The raw data supporting the conclusions of this article will be made available by the authors, without undue reservation.

AUTHOR CONTRIBUTIONS

MJ and SB performed computations. RF and RL discussed the results and wrote the paper. MH designed research and conducted computations and wrote the paper. All authors contributed to the article and approved the submitted version.

FUNDING

MJ thanks the Tunisian Ministry for High Education and Research for a fellowship for the preparation of this work. RF and MH acknowledge financial support from the Swedish Research Council (Sweden). This work was also supported by the CNRS program Physique et Chimie du Milieu Interstellaire (PCMI) co-funded by the Centre National d'Etudes Spatiales (CNES).

ACKNOWLEDGMENTS

This study was undertaken while MH was Waernska Guest Professor at University of Gothenburg (Sweden). The support of this Guest Professorship is hereby gratefully acknowledged. Some of the computations were enabled by resources provided by the Swedish National Infrastructure for Computing (SNIC) at Chalmers Centre for Computational Science and Engineering (C3SE) partially funded by the Swedish Research Council through grant agreement no. 2018-05973.

SUPPLEMENTARY MATERIAL

The Supplementary Material for this article can be found online at: https://www.frontiersin.org/articles/10.3389/fspas.2021.641067/full#supplementary-material

REFERENCES

Adler, T. B., Knizia, G., and Werner, H.-J. (2007). A simple and efficient CCSD(T)-F12 approximation. *J. Chem. Phys*. 127:221106. doi: 10.1063/1.2817618

Ajili, Y., Ben Abdallah, D., Mogren Al-Mogren, M., Francisco, J. S., and Hochlaf, M. (2016). Rotational (de-)excitation of HNS by He: Three-dimensional potential energy surface and collision rate coefficients. *Mon. Not. R. Astron. Soc.* 458, 1581–1589. doi: 10.1093/mnras/stw371

Aliev, M. R., and Watson, J. K. G. (1985). *Molecular Spectroscopy: Modern Research*, Vol. III, edited by K. N. Rao. New York, NY: Academic Press.

Ben Yaghlane, S., Jaidane, N.-E., Cotton, C. E., Francisco, J. S., Mogren Al Mogren, M., Linguerri, R., and Hochlaf, M. (2014). Theoretical spectroscopic investigations of HNS^q and HSN^q (q = 0,+1,-1) in the gas phase. *J. Chem. Phys*. 140:244309. doi: 10.1063/1.4883915

BenYaghlane, S., Cotton, C. E., Francisco, J. S., Linguerri, R., and Hochlaf, M. (2013). Ab initio structural and spectroscopic study of HPS^x and HSP^x (x = 0,+1,−1) in the gas phase. *J. Chem. Phys*. 139:174313. doi: 10.1063/1.4827520

Carbonnière, P., Lucca, T., Pouchan, C., Rega, N., and Barone, V. (2005). Vibrational computations beyond the harmonic approximation: performances of the B3LYP density functional for semirigid molecules. *J. Comput. Chem*. 26, 384–388. doi: 10.1002/jcc.20170

Deegan, M. J. O., and Knowles, P. J. (1994). Perturbative corrections to account for triple excitations in closed and open shell coupled cluster theories. *Chem. Phys. Lett*. 227, 321–326. doi: 10.1016/0009-2614(94)00815-9

Dunning, T. H., Peterson, K. A., and Wilson, A. K. (2001). Gaussian basis sets for use in correlated molecular calculations. X. The atoms aluminum through argon revisited. *J. Chem. Phys*. 114, 9244–9253. doi: 10.1063/1.1367373

Espin, T. E. (1890). Über helle linien im spectrum von R andromedae. *Astronomische Nachrichten* 123:31. doi: 10.1002/asna.18901230106

Fowler, A., and Vaidya, W. H. (1931). The spectrum of the flame of carbon disulphide. *Proc. Roy. Soc. A* 132, 310–330. doi: 10.1098/rspa.1931.0103

Gottlieb, C. A., Ball, J. A., Gottlieb, E. W., Lada, C. J., and Penfield, H. (1975). Detection of interstellar nitrogen sulfide. *Astrophys. J.* 200, L147–L149. doi: 10.1086/181918

Habara, H. S., Yamamoto, and Saito, S. (1998). Microwave spectrum and molecular structure of the H_2NS radical. *J. Chem. Phys.* 109, 2700–2707. doi: 10.1063/1.476876

Hampel, C., Peterson, K., and Werner, H.-J. (1992). A comparison of the efficiency and accuracy of the quadratic configuration interaction (QCISD), coupled cluster (CCSD), and Brueckner coupled cluster (BCCD) methods. *Chem. Phys. Lett.* 190, 1–12. doi: 10.1016/0009-2614(92)86093-W

Hättig, C. (2005). Optimization of auxiliary basis sets for RI-MP2 and RI-CC2 calculations: Core–valence and quintuple-ζ basis sets for H to Ar and QZVPP basis sets for Li to Kr. *Phys. Chem. Chem. Phys.* 7, 59–66. doi: 10.1039/B415208E

Helgaker, T., Klopper, W., Koch, H., and Noga, J. (1997). Basis-set convergence of correlated calculations on water. *J. Chem. Phys.* 106, 9639–9646. doi: 10.1063/1.473863

Hochlaf, M., Puzzarini, C., and Senent, M. L. (2015). Towards the computations of accurate spectroscopic parameters and vibrational spectra for organic compounds. *Mol. Phys.* 113, 1661–1673. doi: 10.1080/00268976.2014.1003986

Irvine, W. M., Senay, M., Lovell, A. J., Matthews, H. E., McGonagle, D., and Meier, R. (2000). Detection of nitrogen sulfide in Comet Hale-Bopp. *Icarus* 143, 412–414. doi: 10.1006/icar.1999.6281

Kendall, R. A., Dunning, T. H. Jr. and Harrison, R. J. (1992). Electron affinities of the first-row atoms revisited. Systematic basis sets and wave functions. *J. Chem. Phys.* 96, 6796–6806. doi: 10.1063/1.462569

Klopper, W. (2001). Highly accurate coupled-cluster singlet and triplet pair energies from explicitly correlated calculations in comparison with extrapolation techniques. *Mol. Phys.* 99, 481–507. doi: 10.1080/00268970010017315

Knizia, G., Adler, T. B., and Werner, H.-J. (2009). Simplified CCSD(T)-F12 methods: Theory and benchmarks. *J. Chem. Phys.* 130:054104. doi: 10.1063/1.3054300

Knizia, G., and Werner, H.-J. (2008). Explicitly correlated RMP2 for high-spin open-shell reference states. *J. Chem. Phys.* 128:154103. doi: 10.1063/1.2889388

Knowles, P. J., Hampel, C., and Werner, H.-J. (2000). Coupled cluster theory for high spin, open shell reference wave functions. *J. Chem. Phys.* 99, 5219–5227. doi: 10.1063/1.465990

Knowles, P. J., and Werner, H.-J. (1985). An efficient second-order MC SCF method for long configuration expansions. *Chem. Phys. Lett.* 115, 259–267. doi: 10.1016/0009-2614(85)80025-7

McGonagle, D., and Irvine, W. M. (1997). Nitrogen sulfide in giant molecular clouds. *Astrophys. J.* 477, 711–721. doi: 10.1086/303749

McGonagle, D., Irvine, W. M., and Ohishi, M. (1994). Nitrogen sulfide in quiescent dark clouds. *Astrophys. J.* 422, 621–625. doi: 10.1086/173755

McKean, D. C., Craig, N. C., and Law, M. M. (2008). Vibrational Anharmonicity and Harmonic Force Fields for Dichloromethane from Quantum-Chemical Calculations. *J. Phys. Chem. A* 112, 10006–10016. doi: 10.1021/jp803881c

Meyer, D. M., and Roth, K. C. (1991). Discovery of interstellar NH. *Astrophys. J. Letters* 376: L49–L52. doi: 10.1086/186100

Millar, T. J., Herbst, E., and Charnley, S. B. (1991). The formation of oxygen-containing organic molecules in the Orion compact ridge. *Astrophys. J.* 369, 147–156. doi: 10.1086/169745

Mills, I. M. (1972). *Molecular Spectroscopy: Modern Research,* edited by K.N. Rao and C.W. Mathews. New York, NY: Academic Press.

Miura, Y., Asada, H., Klnoshita, M., and Ohta, K. (1983). Electron spin resonance study of N-Alkyl-N-(a1kylthio)aminyl Radicals. *J. Phys. Chem.* 87, 3450–4555. doi: 10.1021/j100241a020

Neugebauer, G., Martz, D. E., and Leighton, R. B. (1965). Observations of extremely cool stars. *Astrophys. J.* 142, 399–401. doi: 10.1086/148300

Nguyen, M. T., Vanquickenborne, L. G., and Flammang, R. (1994). The thionitroxyl free radical (H_2NS) and its ionic counterparts (H_2NS^+ and H_2NS^-): a theoretical and experimental study. *J. Chem. Phys.* 101, 4885–4892. doi: 10.1063/1.467410

Pereira, P. S. S., Macedo, L. G. M., and Pimentel, A. S. (2010). New insight into the formation of nitrogen sulfide: a quantum chemical study. *J. Phys. Chem. A* 114, 509–515. doi: 10.1021/jp907384d

Peterson, K. A., Adler, T. B., and Werner, H.-J. (2008). Systematically convergent basis sets for explicitly correlated wavefunctions: the atoms H, He, B–Ne, and Al–Ar. *J. Chem. Phys.* 128:084102. doi: 10.1063/1.2831537

Phuong, N. T., Chapillon, E., Majumdar, L., Dutrey, A., Guilloteau, S., Piétu, V., et al. (2018). First detection of H_2S in a protoplanetary disk. The dense GG Tauri A ring. *A&A* 616:6. doi: 10.1051/0004-6361/201833766

Shamasundar, K. R., Knizia, G., and Werner, H.-J. (2011). A new internally contracted multi-reference configuration interaction method. *J. Chem. Phys.* 135:054101. doi: 10.1063/1.3609809

Strutt, R. J. (1913). An active modification of nitrogen, produced by the electric discharge.—V. *Proc. Roy. Soc. A* 88, 539–549. doi: 10.1098/rspa.1913.0049

Strutt, R. J., and Fowler, A. (1912). Spectroscopic investigations in connection with the active modification of nitrogen. II—Spectra of elements and compounds excited by the nitrogen. *Proc. Roy. Soc. (London) A* 86, 105–117. doi: 10.1098/rspa.1912.0005

Temelso, B., and Shields, G. C. (2011). The role of anharmonicity in hydrogen-bonded systems: the case of water clusters. *J. Chem. Theory Comput.* 7, 2804–2817. doi: 10.1021/ct2003308

Trabelsi, T., Ben Yaghlane, S., Mogren Al Mogren, M., Francisco, J. S., and Hochlaf, M. (2016). HNS^+ and HSN^+ cations: electronic states, spin-rovibronic spectroscopy with planetary and biological implications. *J. Chem. Phys.* 145:084307. doi: 10.1063/1.4961313

Trabelsi, T., Linguerri, R., Ben Yaghlane, S., Jaidane, N.-E., Mogren Al-Mogren, M., Francisco, J. S., and Hochlaf, M. (2015). On the role of HNS and HSN as light-sensitive NO-donors for delivery in biological media. *J. Chem. Phys.* 143:134301. doi: 10.1063/1.4932084

Trabelsi, T., Mogren Al-Mogren, M., Hochlaf, M., and Francisco, J. S. (2018). Mechanistic study of the photoexcitation, photoconversion, and photodissociation of CS_2. *J. Chem. Phys.* 149:064304. doi: 10.1063/1.5040141

van Dishoeck, E. F., Jansen, D. J., Schilke, P., and Phillips, T. G. (1993). Detection of the Interstellar NH_2 Radical. *Astrophys. J. Letters*, 416: L83–L86. doi: 10.1086/187076

Wagenblast, R., Williams, D. A., Millar, T. J., and Nejad, L. A. M. (1993). On the origin of NH in diffuse interstellar clouds. *Mon. Not. R. Astron. Soc.* 260, 420–424. doi: 10.1093/mnras/260.2.420

Weigend, F. (2002). A fully direct RI-HF algorithm: Implementation, optimised auxiliary basis sets, demonstration of accuracy and efficiency. *Phys. Chem. Chem. Phys.* 4, 4285–4291. doi: 10.1039/b204199p

Werner, H.-J., and Knowles, P. J. (1985). A second order multiconfiguration SCF procedure with optimum convergence. *J. Chem. Phys.* 82, 5053–5063. doi: 10.1063/1.448627

Werner, H.-J., and Knowles, P. J. (1988). An efficient internally contracted multiconfiguration–reference configuration interaction method. *J. Chem. Phys.* 89, 5803–5814. doi: 10.1063/1.455556

Werner, H. J., Adler, T. B., and Manby, F. R. (2007). General orbital invariant MP2-F12 theory. *J. Chem. Phys.* 126:164102. doi: 10.1063/1.2712434

Werner, H. J., Knowles, J., et al. (2015). MOLPRO version 2015 is a package of ab initio programs. *University of Cardiff Chemistry Consultants (UC3): Cardiff, Wales, UK*. Available online at: http://www.molpro.net

Westbury, R. A., and Winkler, C. A. (1960). The reactions of active nitrogen with hydrogen sulfide and carbon disulfide. *Can. J. Chem.* 38, 334–342. doi: 10.1139/v60-049

Wöhl, H. (1971). On Molecules in Sunspots. *Solar Phys.* 16, 362–272. doi: 10.1007/BF00162477

Woon, D. E., and Dunning, T. H. Jr. (1993). Gaussian basis sets for use in correlated molecular calculations. III. The atoms aluminum through argon. *J. Chem. Phys.* 98, 1358–1371. doi: 10.1063/1.464303

Xin, J., Fan, H., Ionescu, I., Annesley, C., and Reid, S. A. (2003). Fluorescence excitation spectroscopy of the A^2A_1 - X^2B_1 system of jet-

cooled NH_2 in the region 2900–4300Å. *J. Mol. Spectrosc*. 219, 37–44. doi: 10.1016/S0022-2852(03)00008-0

Yamamura, S. T., Kawaguchi, K., and Ridgway, S. T. (2000). Identification of SH v=1 Ro-vibrational Lines in R Andromedae. *Astrophys. J*. 528, L33–L36. doi: 10.1086/312420

Zen, A., Zhelyazov, D., and Guidoni, L. (2012). Optimized structure and vibrational properties by error affected potential energy surfaces. *J. Chem. Theory Comput*. 8, 4204–4215. doi: 10.1021/ct300576n

Ziurys, L. M. (2006). The chemistry in circumstellar envelopes of evolved stars: Following the origin of the elements to the origin of life. *Proc. Natl. Acad. Sc. U.S.A*. 103, 12274–12279. doi: 10.1073/pnas.0602277103

Conflict of Interest: The authors declare that the research was conducted in the absence of any commercial or financial relationships that could be construed as a potential conflict of interest.